

A Conformational Study of the Hemimercaptal of Methylglyoxal and Glutathione Including the Study of Solvent Effects

María L. Cubas and Oscar N. Ventura*

Cátedra de Química Cuántica, Facultad de Química, C.C.1157,
11800 Montevideo, Uruguay

Received: September 30, 1991

2-Oxopropanal(metilglioal, MG) reage quimicamente com a glutatona reduzida (γ -glutamilcisteinilglicina, GSH) formando um hemimercaptal (HGSH) que age como substrato da enzima Glioalase I (EC 4.4.1.5, Glo I). Um estudo mecânico molecular e semiempírico (AM1 e MNDO-PM3) são apresentados sobre a estrutura do HGSH livre e também cercado por várias moléculas de água a fim de melhor esclarecer sua conformação em solução. Como resultado deste estudo foram determinados os requisitos conformacionais para a reação no centro ativo e é apresentada uma hipótese sobre o mecanismo de reação do enzima.

2-Oxopropanal(methylglyoxal, MG) reacts chemically with reduced glutathione (γ -glutamylcysteinylglycine, GSH) to form a hemimercaptal (HGSH) which acts as the substrate of the Glyoxalase I (EC 4.4.1.5, Glo I) enzyme. A molecular mechanics and semiempirical (AM1 and MNDO-PM3) study is presented here on the structure of HGSH both free and surrounded by several water molecules to get some insight on its conformation in solution. As a result of this model study, the conformational requirements for the reaction at the active center are determined and a hypothesis on the reaction mechanism of the enzyme is presented.

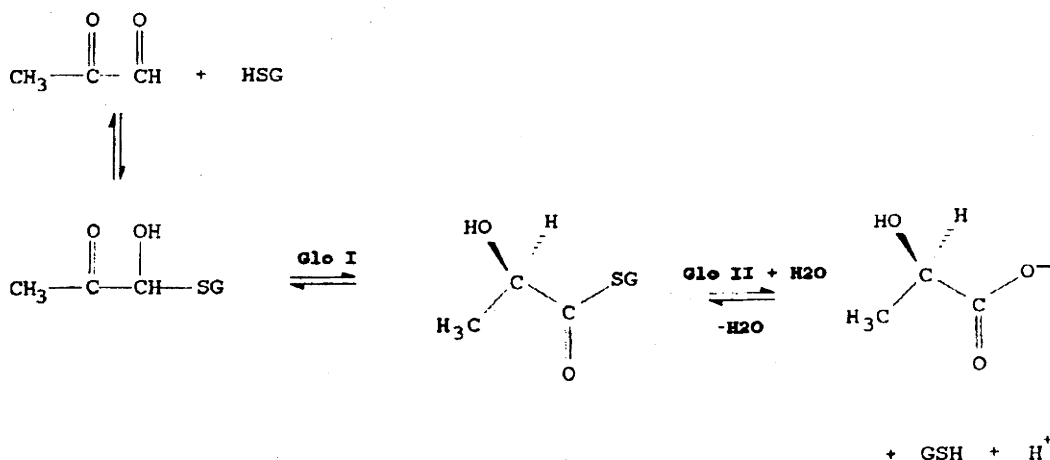
Key words: Methylglyoxal; Glutathione; Glyoxalase; Molecular Mechanics.

Introduction

Several authors have singled out MG as a potential cancerostatic¹. MG is effective as a growth control agent in several biological systems². However, its direct use as a cancerarresting factor has failed, as well as the use of other 2-ketoaldehydes related to MG³. This is due to the existence of the glyoxalase system that rapidly catalyzes the conversion

of 2-oxoaldehydes to the corresponding inactive 2-hydroxyacids⁴.

Glo I acts on the hemimercaptal formed by chemical reaction between MG and GSH⁵. This enzyme is an isomerase which transforms the substrate into S-2-hydroxyacylglutathione⁶. A second enzyme, Glo II, recovers GSH and forms D-lactate by hydrolysis of this thiolester. This reaction



Scheme I

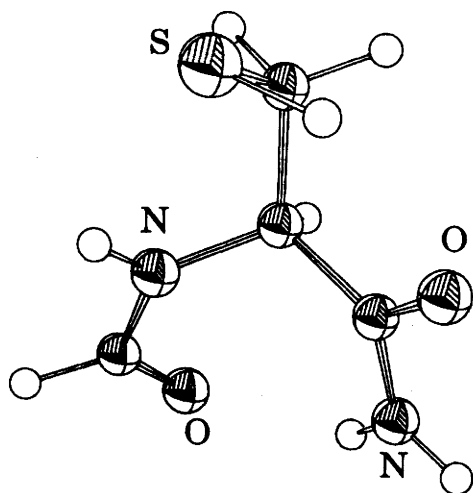


Figure 1. Structure of *n*-formylcysteinamide used as model compound.

mechanism (see Scheme I) is the accepted one since proposed by Racker forty years ago⁷.

Whilst the hydrolysis cause by Glo II is well understood, the mechanism of Glo I has been controversial. Former work on the reaction of Glo I suggest the key step to be a hydride transfer⁸. More recent experimental work however, indicates that a mechanism involving a proton transfer and a enediol intermediate is more likely⁹. The presence of a Zn^{+2} cation coordinated to one or two water molecules at the active center is also known⁹. Chemical modification studies of mammalian Glo I suggested there are one tyrosyl, one tryptophanyl, one lysyl and possibly a glutamyl or aspartyl residues in the active

site. Yeast Glo I instead seems to have cysteinyl, arginyl and tyrosyl residues in the active center.

We have initiated a theoretical study of the mechanism of action of Glo I. We report here a molecular mechanics study on the structure of the hemimercaptal HGSH and a model system, both isolated and surrounded by water molecules as a way of simulating the conditions in solution. Semiempirical calculations of some of the structures considered in this paper were done using the AM1 and MNDO-PM3 approximations. A semiempirical study of the reaction path will be published elsewhere.

Methodology

Molecular Mechanics calculations were done using Allinger's MMP2 method¹⁰ within the PH program¹¹. The simulated annealing method of Kirkpatrick *et al.*¹² was used for positioning each of the water molecules in sequential steps. Full optimization of the intermolecular coordinates (docking) was done after each simulated annealing run. Since HGSH presents three different, strongly solvated areas, each one was studied separately using more water molecules than the necessary for the first solvation shell. The final solvated structure was obtained choosing the H_2O molecules belonging to the first solvation shell in each of the individual studies and resubmitting the whole structure to full optimization. Besides GSH, also a model system, *n*-formylcysteinamide (CAG, Fig. 1), was studied, as well as the hemimercaptals of MG with GSH and CAG (HGSH and HCAG respectively).

Semiempirical calculations were done with the AMPAC¹³ program using the AM1¹⁴ and PM3¹⁵ approximate hamiltonians. Geometry optimizations were done in the standard way using the Broyden-Fletcher-Goldfarb-Shanno algorithm¹⁶.

Results

Two minima are obtained for GSH. One of them is folded due to intramolecular interactions. We consider the contribution of this structure to general behavior of GSH in solution as

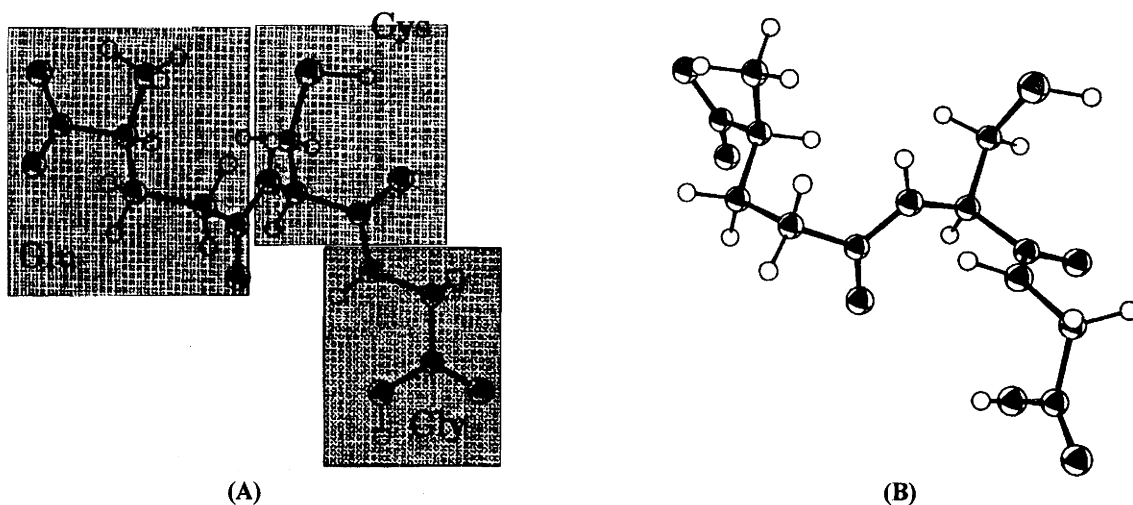


Figure 2. MM optimized unfolded structure of glutathione (A) and crystallographic structure (B).

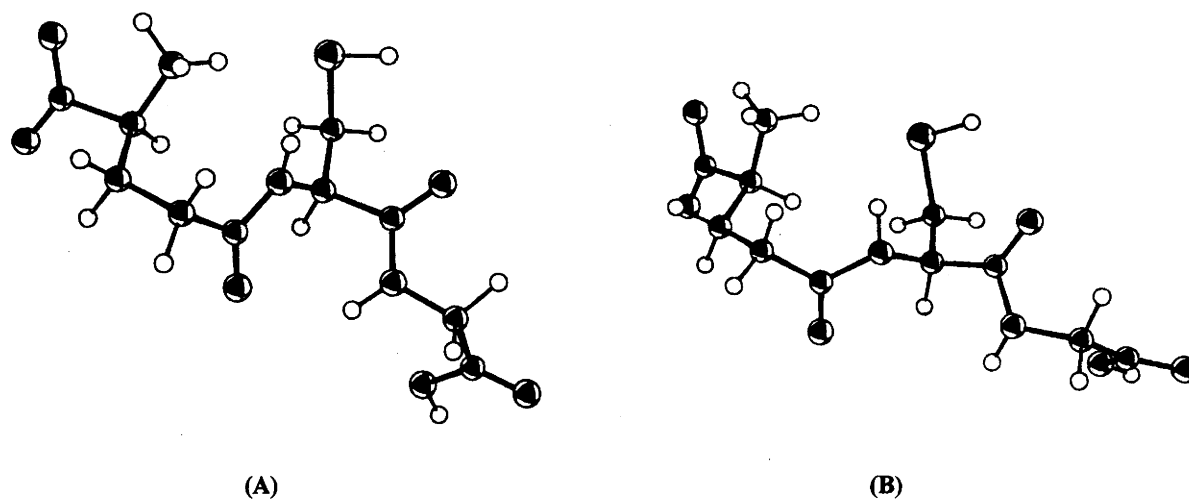


Figure 3. AM1 (A) and PM3 (B) optimized unfolded structure of glutathione.

negligible because solvation would open the structure by hydrogen bonding to solvent molecules. The second structure is an unfolded one (Fig. 2). It is a secondary minimum for isolated GSH by 14.5 kcal/mol at the MM level. As quoted in a previous paper¹⁷, this conformer is generally coincident with the crystallographically determined structure of GSH¹⁸. The main differences are found in some of the torsion angles of the zwitterionic group, the glycine terminal acid group and the amide group. This last one is very sensible to the environment, as was later proved by formation of the hemimercaptal and by solvation. We do not consider these differences significant, since they are probably due to the difference between the isolated GSH and the molecule immersed in the crystal field. However, better force fields designed specifically for peptides are able to predict a theoretical structure very similar to the experimental one¹⁹. Further discussion on these points can be found in the above mentioned paper¹⁷.

To obtain a more quantitative assessment of the energy difference between the conformers, semiempirical geometry optimization of both structures was done. The folded structure given by those methods (Fig. 4) is generally coincident with the folded MMX one and is the global minimum both for AM1 and PM3. The unfolded structures however, do not reproduce satisfactorily the crystallographic data due to intramolecular interactions between the zwitterionic group and sulfide on one side and the glycine group and the thiolic hydrogen on the other (Fig. 3). The difference in heats of formation between both conformers was evaluated as 9.2 kcal/mol at the AM1 level and 5.6 kcal/mol at the MNDO-PM3 one. The three methods indicate thus the necessity of solvation for stabilizing the completely unfolded conformation of glutathione.

Three different MM2 minima were found for HCAG (Fig. 5). Two of them are considered as most likely to be present in solution (conf. I and II, Fig. 5). The most significant difference between these last two conformers is the dihedral angle of the $-\text{COCH}_3$ group of MG. Enthalpies at each level of calculation are reported in Table 1.

The most important feature of the HCAG structure is an interfragment hydrogen bond between and $-\text{OH}$ in the MG residue and a carbonyl group in one of the amide bonds of the CAG residue. This H-bond is maintained, as expected, in the HGSH structures, shown in Fig. 6. There is, however, an im-

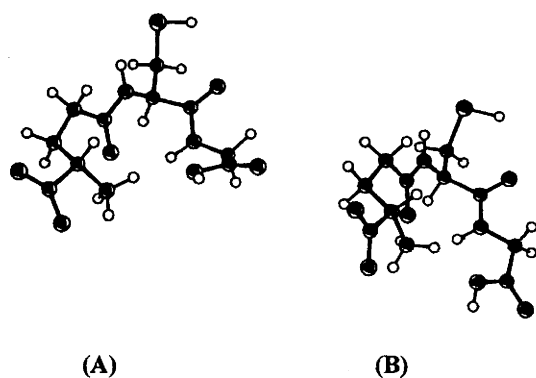


Figure 4. AM1 (A) and PM3 (B) global minima of glutathione (correspond to the MM folded global minimum).

Table 1. Stability of the three main conformers of HCAG according to the methods used in this paper. Enthalpies in kcal/mol.

Method	Conf. I	Conf. II	Conf. III
MMX	-202.0	-198.7	-208.7
AM1	-163.3	-161.0	-164.3
PM3	-153.4	-151.7	-154.4

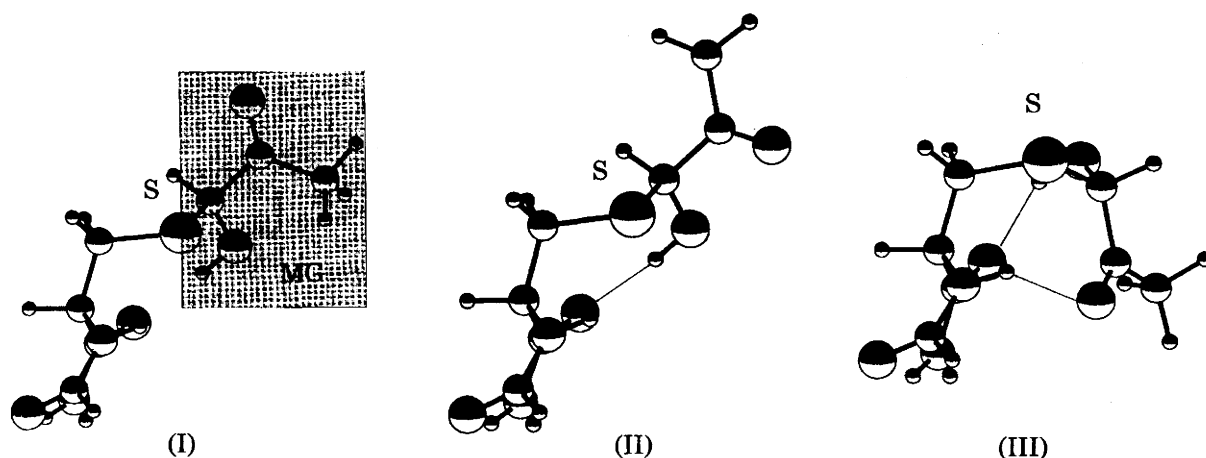


Figure 5. MM optimized structures of three different conformers of the hemimercaptal of *n*-formylcysteinamide and methylglyoxal. The corresponding energies for these structures are reported in Table I (from left to right, conf. I, II and III respectively). The MG fragment is highlighted in the first structure. The interfragment H-bond is shown in the second and third structure. The interfragment H-bond is shown in the second and third structures. An extra stabilizing H-bond is also shown in the folded structure.

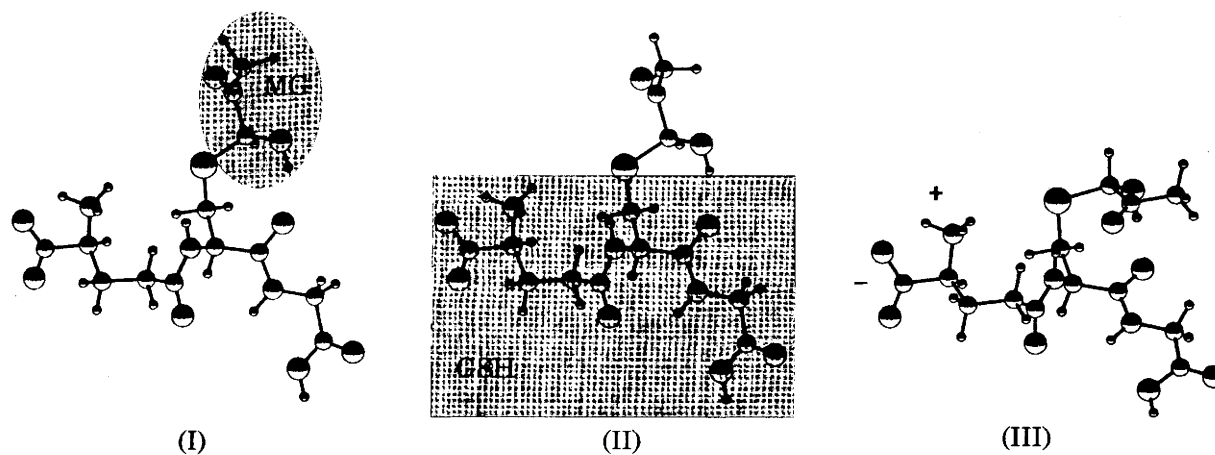


Figure 6. The three conformers of the hemimercaptal of GSH and MG, corresponding to the three conformers of HCAG in Fig. 5. The MG and GSH fragments are marked in structures I and II, while the charges on the molecule are indicated in structure III.

portance difference between the HCAG and HGSH structures with respect to this hydrogen bond. In fact, it is more labile in HCAG than in HGSH; a water molecule can disrupt this H-bond in the first structure (see Fig. 7), but it is unable to do so in HGSH (see later on). This larger stability of the H-bond in HGSH with respect to HCAG is attributed to the effect of the zwitterionic terminal group in the former. Correspondingly, the energy difference between the conformers is reduced, as show in Table 2.

A second important point concerning the above-mentioned hydrogen bond is that it contributes to fix the Hc atom in the opposite face of the molecule with respect to the oxygens

Table 2. MMX stability of the three main conformers of the memimercaptals. HGSH solv refers to the solvated conformers as shown in Fig. 12. Enthalpies in kcal/mol.

	Conf. I	Conf. II	Conf. III
HCAG	-3.3	0.0	-10.
HGS	-1.3	0.0	-3.7
HGSH	-7.0	0.0	---

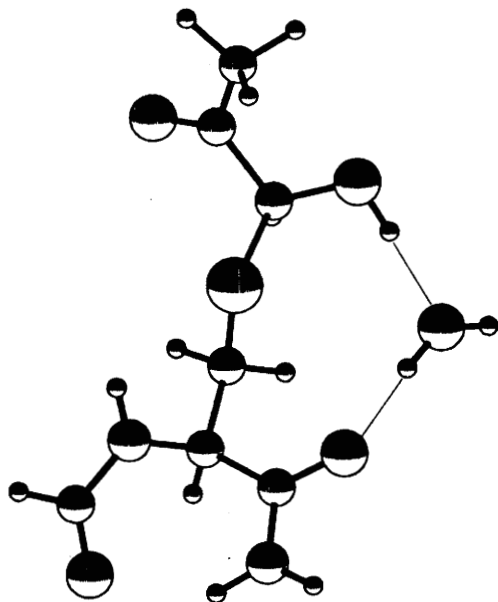


Figure 7. Optimized structure of HCAG with one water molecule, demonstrating how there is the possibility of disruption of the intramolecular H-bond in HCAG by a solvent molecule.

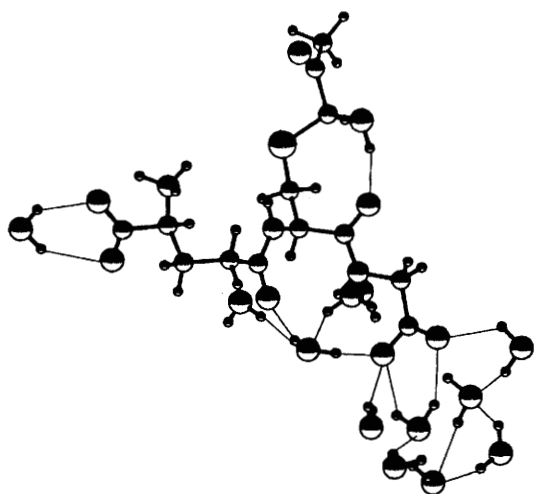


Figure 8. Structure of the solvation shell around the deprotonated glycine residue in HGSH.

which will participate in the reaction. Since the abstraction of this proton is the initial step in the proposed mechanism, it is encouraging to find that the minimum structure has it positioned in a convenient way for this abstraction.

In physiological conditions the glycine residue of GSH is deprotonated²⁰. This is the first solvation site of GSH and, consequently, also HGSH. The second site is the zwitterionic end while the third is the MG residue. Three experiments were conducted for studying the solvation of HGSH. In the first place, the glycine residue was deprotonated (physiological

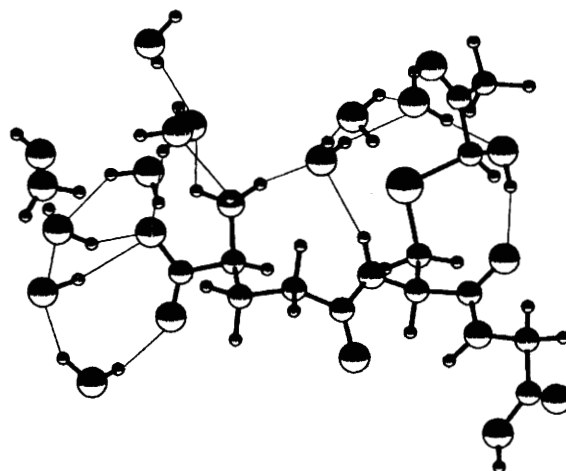


Figure 9. Structure of the solvation shell around the zwitterionic end of HGSH.

conditions) and the water molecules clustering around it were investigated (see Fig. 8). Secondly, the glycine residue was left protonated and the water molecules clustering around the zwitterionic end were considered (Fig. 9). Finally, we considered a structure of HGSH where both ends were left out but the -NH_4^+ group was kept (Fig. 10). This structure allowed us to study separately the solvation of the MG residue, but keeping the influence of the zwitterionic end on the interfragment hydrogen bond so that it does not break when the complexation with water occurs. The whole HGSH, but with both acid groups protonated, was also employed for this purpose, giving the same results. This demonstrates thus that the simplification

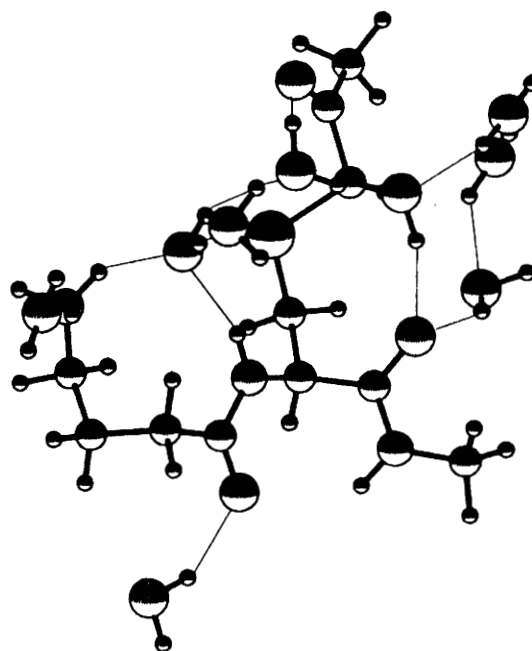


Figure 10. Structure of the solvation shell around the MG fragment of HGSH.

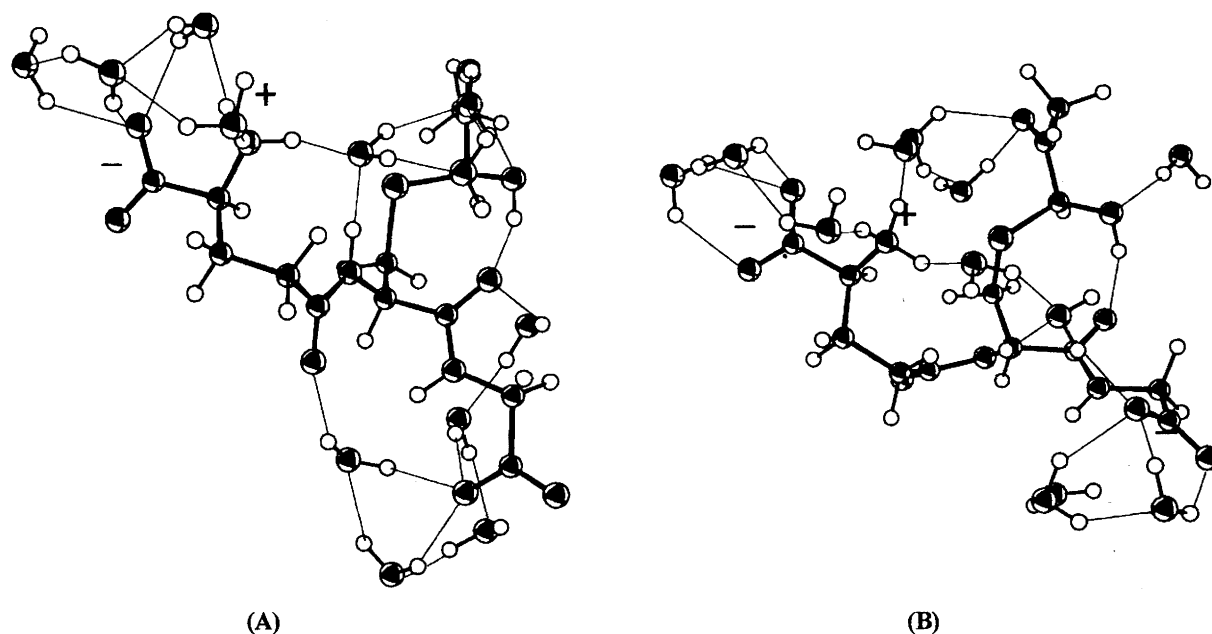


Figure 11. Optimized structure of both more likely conformers of HGSH in solution showing the most important waters of solvation.

of the model structure is valid. In all these figures only one of the conformers of the HGSH structure is shown.

One can notice that several positions of the water molecules in each of the experiments are repeated in the other ones. Also, not all the H₂O molecules participate in the first solvation shell. These molecules were discarded in the final structure studied. The final optimized solvated structures for the two unfolded conformers of HGSH are shown in Fig. 11. In these structures one sees first that the interfragment H-bond is not broken in any case by a solvent water molecule. Second, the structure of the solvent cage affects the conformation of HGSH. Moreover, this cage transmits the influence of the change in conformation of the MG fragment to the peptide backbone (which has a different conformation in both conformers, contrary to the case when water was absent). Third, at least in one of the conformers the most important complexed water at the MG fragment links both oxygens.

Using all the above facts a hypothesis was elaborated as to the structure of the active site. From the optimum structures obtained for the isolated HCAG and HGSH we postulate that the interfragment hydrogen bond is essential for defining two faces on the MG residue: one where both reactive oxygens are located and the other from which the proton is to be abstracted. Furthermore, the fact that water effectively stabilizes the unfolded minimum lends support to the idea that both ionic ends of the GSH residue in HGSH not only act as anchors of HGSH to Glo I, but they are also important in defining the local geometry of the MG residue. These two anchoring points plus the interaction of the face containing the oxygen of the MG residue (OO face) with the active site of the enzyme provide the stabilization for the initial complex enzyme-substrate.

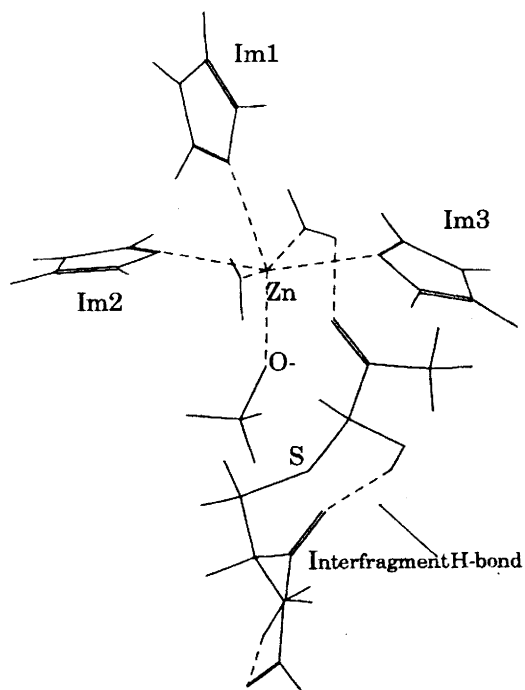


Figure 12. Model complex between the active center built using experimental data and one of the conformers of HCAG as determined in this paper.

Furthermore, from the data obtained in the solvation studies it is clear that one molecule of water may be located over the OO face with both hydrogens interacting with the oxygens of the MG residue. Since from some experimental work it was concluded that there must be a water molecule in between the substrate and the Zn^{+2} cation, we here postulate that water molecule to be the one coordinated to the Zn^{+2} ion in the enzyme-substrate complex. A graphic representation of the complex between a simulated active center (built using EXAFS data) and the optimized structure of HGSH is shown in Fig. 12. A semiempirical study of the reaction path for the obtention of the enediol intermediate will be published elsewhere²¹.

Supplementary material

Coordinates and energies for the optimized structures are available from the authors.

Acknowledgements

Support from the Commission of the European Communities under contract CII.0625.UY and from the UNDP under contract URU/84/002-Pedeciba are gratefully acknowledged.

References

1. A. Szent-Györgyi, A. Hegyeli, J.A. McLaughlin, *Science* **140**, 1391-1392 (1963); A. Szent-Györgyi, *Electronic Biology and Cancer*, M. Dekker, New York, 1976.
2. A. Szent-Györgyi, L. G. Egyud, J. A. McLaughlin, *Science* **155**, 539-541 (1967).
3. G. Fodor, R. Mujumdar, J. Butterick, *Ciba Found. Symp.* **67**, 165-174 (1979); P.J. Conroy, *Ciba Found. Symp.* **67**, 271-300 (1979).
4. H.D. Dakin, H.W. Dudley, *J. Biol. Chem.* **14**, 155-157 (1913); C. Neuberger, *Biochem. Z.* **49**, 502-506 (1913); see ref. 22 for a modern review of this subject.
5. S. Sellin, A.-C. Aronsson, L.E.G. Eriksson, K. Larsen, G. Tibbelin, B. Mannervik in *Functions of Glutathione: Biochemical, Physiological, Toxicological and Clinical Aspects*, A. Larsson *et al.* (eds), Raven Press, New York, 1983, pp 187-197.
6. S. Sellin, B. Mannervik, *J. Biol. Chem.* **258**, 8872-8875 (1983).
7. E. Racker, *J. Biol. Chem.* **190**, 685-696 (1951).
8. D. L. Vander Jagt, L. -P. B. Han, *Biochemistry* **12**, 5161-5167 (1973).
9. J. W. Kozarich, R. V. J. Chari, J. C. Wu, T. L. Lawrence, *J. Am. Chem. Soc.* **103**, 4593-4594 (1981); A. -C. Aronsson, E. Marmstål, B. Mannervik, *Biochem. Biophys. Res. Commun.* **81**, 1235-1240 (1978); S. Sellin, P. R. Rosevear, B. Mannervik, A. S. Mildvan, *J. Biol. Chem.* **257**, 10023-10029 (1982); P. R. Rosevear, R. V. J. Chari, J. W. Kozarich, S. Sellin, B. Mannervik, A. S. Mildvan, *J. Biol. Chem.* **258**, 6823-6826 (1983); S. Sellin, B. Mannervik, *J. Biol. Chem.* **259**, 11426-11429 (1984); L. Garcia-Iniguez, L. Pomes, B. Chance, S. Sellin, B. Mannervik, A. S. Mildvan, *Biochemistry* **23**, 685-689 (1984); S. S. Hall, A. M. Doweyko, F. Jordan, *J. Am. Chem. Soc.* **98**, 7460-7461 (1976).
10. U. Bukert, N. L. Allinger, in *Molecular Mechanics*, M. C. Caserio (ed), A. C. S. Monography 177, American Chemical Society, Washington, DC, 1982; N. L. Allinger, Y. H. Yuh, *MM2, Program 395*, Quantum Chemistry Program Exchange, Department of Chemistry, Indiana University, Bloomington, Indiana, USA.
11. PH program, Serena Software, based on C. Still's MODEL program for the VAX machine.
12. S. Kirkpatrick, C. Gelatt, M. Vecchi, *Science* **220**, 671-680 (1983).
13. M. J. S. Dewar, J. J. P. Stewart, M. Eggar, AMPAC, *Program 527*, Quantum Chemistry Program Exchange, Department of Chemistry, Indiana University, Bloomington, Indiana, USA.
14. M. J. S. Dewar, E. G. Zoebisch, E. F. Hraly, J. J. P. Stewart, *J. Am. Chem. Soc.* **107**, 3902 (1985).
15. J. J. P. Stewart, *J. Comput. Chem.* **10**, 209, 221 (1989).
16. C. G. Broyden, *J. Inst. Mathem. Appl.* **6**, 222 (1970); R. Fletcher, *Comput. J.* **13**, 317 (1970); D. Goldfarb, *Mathem. Comput.* **24**, 23 (1970); D. F. Shanno, *Mathem. Comput.* **24**, 647 (1970); D. F. Shanno, *J. Optim. Theory Appl.* **46**, 87 (1985).
17. M. Paulino-Blumenfeld, N. Hikichi, M. Hansz, O.N. Ventura, *J. Mol. Struct. Theochem.* **210**, 467-475 (1990).
18. C. H. Görbitz, *Acta Chem. Scand.* **B41**, 362-366 (1987).
19. S. Wolfe, D. F. Weaver, K. Yang, *Can. J. Chem.* **66**, 2687-2702 (1988).
20. D. L. Rabenstein, *J. Am. Chem. Soc.* **95**, 2997-2803 (1973); S. Fujiwara, G. Formicka-Kozłowska, H. Kozłowski, *J. Chem. Soc. Japan* **50**, 3131-3135 (1977); T. N. Huckerby, A. J. Tudor, *J. Chem. Soc. Perkin II*, 759-763 (1985).
21. M. L. Cubas, O. N. Ventura, *Int. J. Quantum Chem.*, to be published.
22. P. J. Thornalley, *Biochem. J.* **269**, 1-11 (1990).